Pergamon

Phys. Chem. Earth, Vol. 21, No. 5–6, pp. 463–469, 1996

0079-1946/96 $15.00 + 0.00

PII: S0079-1946(97)00059-1

^{18}O in Atmospheric CO_2 Simulated by a 3-D Transport Model: A Sensitivity Study to Vegetation and Soil Fractionation Factors

P. Peylin[1], P. Ciais[1], P. P. Tans[2], K. Six[2], J. A. Berry[3] and A. S. Denning[4]

[1] LMCE, Laboratoire de Modélisation du Climat et de l'Environnement, CE Saclay, Bat 709, Orme des Merisiers, F-91191 Gif sur Yvette Cedex, France
[2] Max-Planck Institut fur Meteorologie, Bundestrasse 55, Hamburg, Germany
[3] Carnegie Institution of Washington, Department of Plant Biology, Stanford, CA, USA
[4] Colorado State University, Department of Atmospheric Sciences, Fort Collins, CO, USA

Received 28 October 1996; accepted 8 January 1997

Abstract. The $^{18}O/^{16}O$ ratio in atmospheric CO_2 is a signal dominated by the processes by which the global land biosphere absorbs and respires CO_2. Potentially it makes it possible to separate the photosynthesis from the total ecosystem respiration provided that leaf CO_2 and soil CO_2 have different isotopic signatures, that the air-sea exchange is correctly treated and that the isotopic value of anthropogenic emissions is well characterized. In this paper we simulate the $\delta^{18}O$ of atmospheric CO_2, using the 3-D tracer model TM2. We perform a specific sensitivity study of $\delta^{18}O$ to the fractionation factors for the diffusion of CO_2 out of the soils (ϵ_{soil}) and into/out of the leaves (ϵ_{leaf}). The control run is similar to Ciais et al. (1996a). The latitudinal gradient, the seasonal amplitude in the northern hemisphere and the mean long term trend appear to be fairly sensitive to these two factors. The trend is nevertheless the most sensitive but it also highly depend on the atmospheric $\delta^{18}O$ mean value and on the stratospheric enrichment of ^{18}O in CO_2 pertaining to the photolysis of O_3.

1 Introduction

An increasing attention has been given to the isotopes of CO_2 ($^{13}CO_2$ and more recently $C^{18}O^{16}O$), as they bring additional constrains to the global carbon cycle. The oxygen isotopic content of atmospheric CO_2 is primarily driven by interactions between CO_2 and the reservoirs of liquid water (see Eq. 2 in Table 1 for isotopic equilibrium between CO_2 and H_2O). Francey and Tans (1987) showed indeed that direct O atom exchange between CO_2 and H_2O vapor does not occur in the gas phase. On the other hand, when CO_2 dissolves in water, an isotopic equilibrium for oxygen atoms takes place. Because the amount of water available is huge compared to the amount of CO_2, the $^{18}O/^{16}O$ ratio in CO_2 is determined by the one of water at a given temperature. Francey and Tans (1987) and Farquhar et al. (1993) pointed out the major influence of CO_2 exchanges with leaf water (photosynthesis) and soil water (soil respiration). Ciais et al. (1996a,b) further tested these parameterizations in a global 3-D transport model, and obtained reasonable agreement between simulated and observed $^{18}O/^{16}O$ ratio in atmospheric CO_2. Following their work, we present here a sensitivity study of this ratio to the fractionation factors involved during the diffusion of CO_2 out of the soil and into/out of the leaves.

Correspondence to: P. PEYLIN

2 The observations

^{18}O in CO_2 is routinely measured at specific locations around the world from three independent air sampling networks: the NOAA-CU network of 17 sites (Trolier et al., 1996), the SCRIPPS-CIO network of 10 sites (*Meijer et al.*, in preparation), and the CSIRO network of 5-6 sites (Francey et al., 1990). The $^{18}O/^{16}O$ isotopic ratios are reported in the δ scale (Eq. 1, Table 1), and $\delta^{18}O$ values are expressed in per mil (‰). At a global scale, three major features can be retrieved from the atmospheric observations.

1. A *north minus south difference* of roughly -1.5‰: the northern hemisphere is permanently depleted in ^{18}O, as first observed by Francey and Tans (1987).
2. A strong *seasonal cycle* at high northern latitudes (Keeling, 1961): there is a maximum in early summer and a minimum in early winter. The observed peak-to-peak amplitude is 1.44‰ at Point Barrow (71°N, 156°W) while Cape Grim in the southern hemisphere (40°S, 140°E) has a lower peak-to-peak amplitude of 0.4‰.
3. The long time series of the SCRIPPS-CIO network (5 sites since 1977) shows *no long term trend* in the

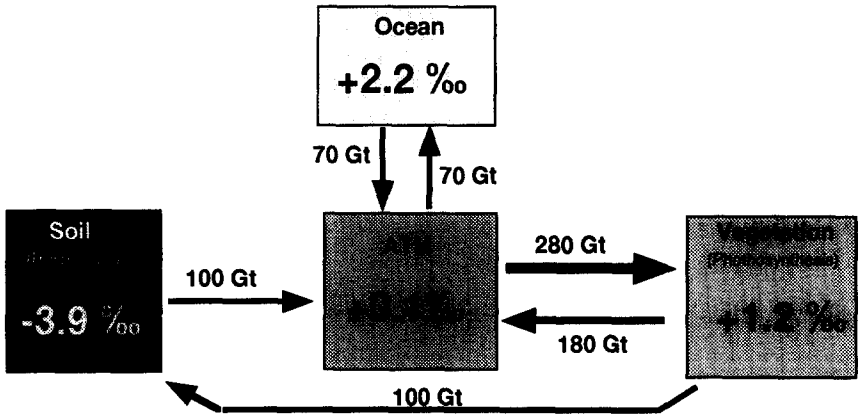

Fig. 1. The global "pre-anthropogenic" exchange fluxes of CO_2 (in GTC (10^{15} g) yr^{-1}) between the atmosphere and the terrestrial biosphere and the ocean, as well as the isotopic composition of CO_2 (expressed in ‰ PDB-CO_2), in equilibrium with the exchangeable water. The $\delta^{18}O$ value of these three reservoirs is weighted in space and time with the exchange fluxes.

mean atmospheric $\delta^{18}O$ (e.g., record at Mauna-Loa, Meijer et al., private communication).

Exchange with leaves and soils is strongly seasonal over temperate and boreal ecosystems which likely account for most of the observed $\delta^{18}O$ annual cycle. Moreover the combined effects of photosynthesis and respiration tend to decrease the local $\delta^{18}O$ in atmospheric CO_2 at high northern latitudes. This pattern follows the composition of precipitation which is depleted in ^{18}O relative to sea-water towards high latitudes and towards the interior of continents.

3 Biospheric fluxes

We coupled the surface exchange fluxes of CO_2 and $C^{18}O^{16}O$ for each reservoir to an atmospheric 3-D tracer model (TM2) in order to simulate the global distribution of $\delta^{18}O$ in atmospheric CO_2. The TM2 model (Heimann, 1995) uses atmospheric forcing from ECMWF in Reading (UK) and it is run at a resolution of 7.5° by 7.5° in the horizontal, with 9 vertical levels (σ coordinates). We will focus on the global "pre-anthropogenic" steady state budget of $\delta^{18}O$ in atmospheric CO_2 and more specifically on the terrestrial biospheric fluxes. Figure 1 presents the CO_2 gross exchange fluxes between the atmosphere and the vegetation, the soils and the ocean, as well as the $\delta^{18}O$ of CO_2 in isotopic equilibrium with chloroplast water, soil water or sea surface water. The main equations used to describe these processes are reported in Table 1.

- *Leaf exchange* : During photosynthesis, all of the atmospheric CO_2 that enters the chloroplasts, isotopically equilibrates with the evaporating water, in presence of enzyme Carbonic Anhydrase. Some of the CO_2 is then assimilated by photosynthesis (net Assimilation, A) but more than half of it diffuses back to the atmosphere. Chloroplast water is enriched in ^{18}O compared to soil water because heavier water molecules evaporate less efficiently than the lighter ones. The degree of enrichment of leaf water is sensitive to the relative humidity, the canopy temperature and to $^{18}O/^{16}O$ ratio in water vapor (Craig and Gordon, 1965). It can be thus highly variable in space and time: the Assimilation weighted mean value in our simulation is +1.2‰ (Fig. 1). Moreover $C^{18}O^{16}O$ diffuses more slowly than $C^{16}O_2$ into/out of the leaves (coefficient α_l in equation 3, Table 1). The overall effect of photosynthesis is to increase the $\delta^{18}O$ in atmospheric CO_2.

- *Soil exchange* : The decomposition of dead organic matter by soil microorganisms and root respiration in the soil produce CO_2 which diffuses up to the atmosphere. This net flux augmented by the stem and twigs respiration, balances on annual mean the net uptake of CO_2 during photosynthesis. We thus neglect any net carbon storage or loss by ecosystems on an annual mean basis. Diffusion in the soil is likely slow enough for CO_2 to fully exchange ^{18}O with the water at the soil surface, even without Carbonic Anhydrase (Ciais et al., 1996a). The $^{18}O/^{16}O$ ratio of soil water tends to follow the variations in surface soil moisture, and thereof the precipitation. This leads in our simulation to a respiration weighted mean value of -3.9‰ for CO_2 isotopically equilibrated with soil water (Fig. 1). As for leaf exchange, a diffusive fractionation occurs during diffusion of CO_2 out of the soil (coefficient α_s in equation 4, Table 1), and the effect of soil respiration is to decrease the $\delta^{18}O$ in atmospheric CO_2.

- *Ocean exchange* : The net CO_2 flux between the ocean and the atmosphere can be split in two gross (one way) fluxes (equation 5, Table 1). The CO_2 gross flux out of the ocean is assumed to be isotopically equilibrated with sea-water, according to reaction (2). The $\delta^{18}O$ of sea-surface water is computed from the sea-surface temperature and the salinity, as in Farquhar et al. (1993). The fractionation during CO_2 diffusion at the air-sea interface is very small (-0.8‰) and the global effect of air-sea exchange is to increase the atmospheric $\delta^{18}O$ value (Fig. 1).

- *Stratospheric enrichment*: Recent measurements of $\delta^{18}O$ of CO_2 reported by Gamo et al. (1989) showed a mass independent enrichment in ^{18}O of 2‰ in the lower stratosphere (19 km) relative to the mean tropospheric value. This enrichment increases with altitude and pertains to the photolysis of O_3 in the stratosphere (Yung et al., 1991). We parameterized this effect by simply adding a source of $C^{18}O^{16}O$, constant in time and space in the upper two levels of the transport model in order to simulate a mean vertical profile of $\delta^{18}O$ of CO_2 close to that observed (Fig. 4).

The CO_2 gross fluxes between the atmosphere and the vegetation (F_{la} and F_{al}, Table 1) are derived from the SIB2 land-surface parameterization (Sellers et al., 1986, 1996; Randall et al., 1996) coupled to the CSU-GCM (Randall et al., 1992; Randall and Pan, 1993; Fowler et al., 1996). The total respiration (F_{resp}, Table 1) equals the net assimilation of carbon over a year but it is distributed in time according to the ground moisture and soil temperature. The oceanic gross fluxes (F_{oa} and F_{ao}, Table 1) are calculated using ΔpCO_2 from the Hamburg Model of the oceanic carbon cycle (Maier-Reimer, 1993; Six and Maier-Reimer, 1996), and gas exchange coefficients derived from ECMWF 10 meter wind fields. These coefficients follow the Liss and Merlivat relationship (Liss and Merlivat, 1986) and they are scaled by a global factor of 1.9 in order to be consistent with the global inventory of ^{14}C in the ocean. The monthly means $\delta^{18}O$ of precipitation are taken from the GISS simulations (Jouzel et al., 1987). We run the tracer model for each component described above and with the atmospheric wind fields corresponding to the period 1990-1994. The choice of this particular period has no importance regarding the mean budget of $\delta^{18}O$ in CO_2. The specific $\delta^{18}O$ field relative to one process can be then calculated. But as the δ fields are not additive we use the δ-anomalies (δ^*, defined in Eq. 1, Table 1) which are additive, in order to combine and compare several components (Fig. 2-3).

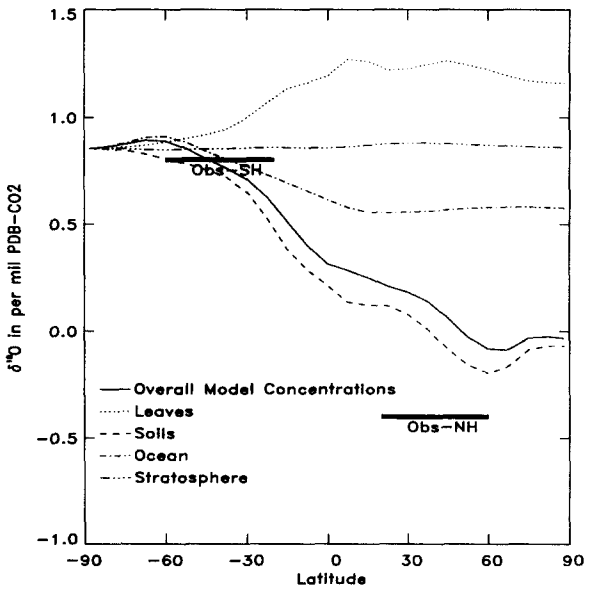

Fig. 2. Simulated $\delta^{18}O$-anomalies (δ^*, see equation 1, Table 1) of atmospheric CO_2 at the surface using the 3-D transport model TM2 (zonal average). The different components correspond to the separate $\delta^{*18}O$ implied by leaf exchange, soil exchange, ocean exchange and stratospheric enrichment. The observations represent the mean value between 20° and 60° for the northern hemisphere and between 20° and 60° for the southern one (derived from a zonal fit to the observations made by the NOAA-CU network).

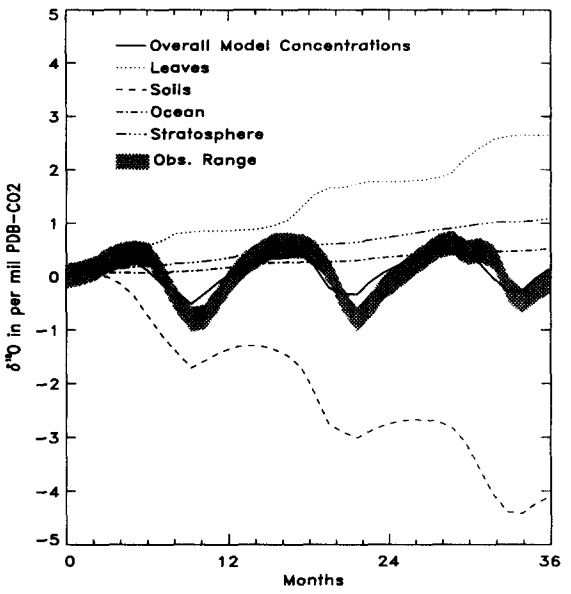

Fig. 3. Simulated $\delta^{18}O$-anomalies (δ^*) in atmospheric CO_2 simulated at Point Barrow (71°N, 156°W) for the period 1990 to 1993. The different components are as in Fig. 2. The grey region represent the observations from the NOAA-CU network (the range is two times the standard deviation of the function used to fit the observations).

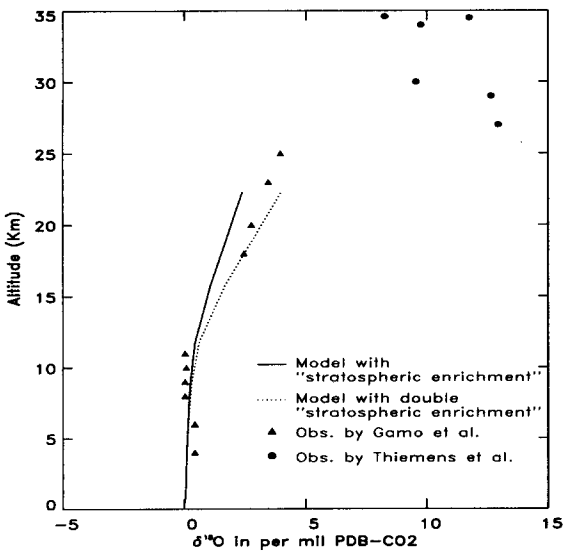

Fig. 4. Simulated δ^{18}O-anomalies (δ^*) in atmospheric CO_2 averaged over all grid points (vertical profile). The dot curve corresponds to a simulation where the "stratospheric enrichment" is double compared to the control run (solid line). Triangles are data by Gamo et al. (1989) over Japan and circles by Thiemens and Jackson (1991) over Palestine.

4 Sensitivity of δ^{18}O in CO_2 to fractionation factors

4.1 Control run

Ciais et al. (1996b) realized a simulation of δ^{18}O in atmospheric CO_2 over the course of a year. Their results fit reasonably well the observations in terms of north minus south difference and seasonal amplitudes at the Point Barrow, Mauna-Loa and Cape Grim stations. We use in this study a slightly different control run. The CO_2 exchange coefficient for the oceanic fluxes (Kex in equation 5, Table 1) is derived from Liss and Merlivat relationship instead of from the stability dependent theoretical formulation of Erickson (1993). We also included the stratospheric enrichment of ^{18}O in CO_2, for the "pre-industrial" scenario.

Figure 2 plots the zonal average of the simulated δ^{18}O-anomalies (δ^*) at the surface. It shows the relative contribution of the terrestrial biosphere and of the ocean and the opposite effect of vegetation and soils. The simulated north-south gradient is compared to an estimate of the observed difference between the northern and the southern hemisphere (see caption, Fig. 2). This control run with only the "pre-industrial" fluxes explain a large part of the observed difference, although the additional depletion of the $^{18}O/^{16}O$ ratio in CO_2 due to fossil fuel burning is missing in this scenario.

Figure 3 presents the simulated trend in δ^{18}O-anomalies (δ^*) at Point Barrow (71°N, 156°W) for each components as well as the observations from the NOAA-CU network. The trend is primarily determined by the biospheric exchanges, while the ocean plays a weaker role. There is a competing effect between soils and vegetation for the net budget of ^{18}O in atmospheric CO_2. While the ecosystem global respiration depletes the atmospheric CO_2 in ^{18}O, the photosynthesis enriches it. Ciais et al. (1996b) used only a global formulation similar to equation 6 (Table 1). They solved this global equation for the parameter α_s to obtain a zero trend for δ^{18}O in atmospheric CO_2. In our simulation, we verified that with the TM2 model such an approach gives similar results if we compare the real trend simulated at many locations and the one calculated through the global budget.

Concerning the "pre-anthropogenic" steady state budget for ^{18}O in CO_2 we would like to simulate a long term trend close to zero as well as realistic inter-hemispheric difference and seasonal amplitude at Point Barrow. Even if the exchange time for the oxygen atom in CO_2 with the biosphere was estimated by Farquhar et al. (1993) to be much smaller than with the ocean (2.2 and 8.3 years respectively), the two reservoirs are connected to each other by the mean atmospheric δ^{18}O level. At long time-scales both reservoirs will thus contribute to the mean δ^{18}O value. Concerning the biosphere, the δ^{18}O fluxes (Eqs. 3-4, Table 1) are driven mainly by the CO_2 gross exchanges fluxes (F_{resp}, F_{al}, F_{la}), the isotopic ratio of water in isotopic equilibrium with CO_2 and the fractionation during the diffusion of CO_2 (α_s and α_l). In the following, we specifically analyze the sensitivity of δ^{18}O in atmospheric CO_2 to the two fractionation factors.

4.2 Sensitivity to the fractionation factors ϵ_s and ϵ_l

Figure 5 presents the results of three sensitivity tests where the two fractionation factors $\epsilon_s = (\alpha_s - 1) \cdot 10^3$ and $\epsilon_l = (\alpha_l - 1) \cdot 10^3$ vary over a given physical range (the other parameters were set as in the control run). These tests were performed with only one simulation. We multiplied the concentration fields produced by the transport model (TM2) with the desired ϵ_s and ϵ_l coefficients. This is possible because these coefficients only scale the ^{18}O fluxes (Eqs. 3-4, Table 1) and because the concentration fields produced by TM2 for each component are additive. The first plot (Fig. 5a) presents the δ^{18}O trend in atmospheric CO_2 at Point Barrow. Because of the relatively short mixing time for CO_2 in the atmosphere, the trend at this station represents well the mean atmospheric trend, when sources and transport are at steady state. We realized the same sensitivity test for the seasonal amplitude at Point Barrow (Fig. 5b) and for the global difference between the northern hemisphere and the southern hemisphere (Fig. 5c: difference calculated as in Fig. 2). In grey we shade the region that corresponds to realistic "observed" values for the three quantities. We made the assumption that

a steady state was reached at "pre-industrial" time with a long term trend close to zero and that the amplitude of the seasonal cycles has not significantly changed compared to the actual observations.

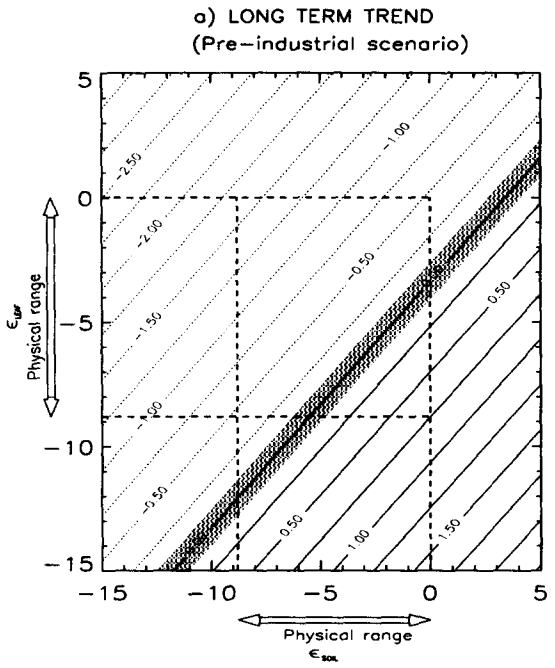

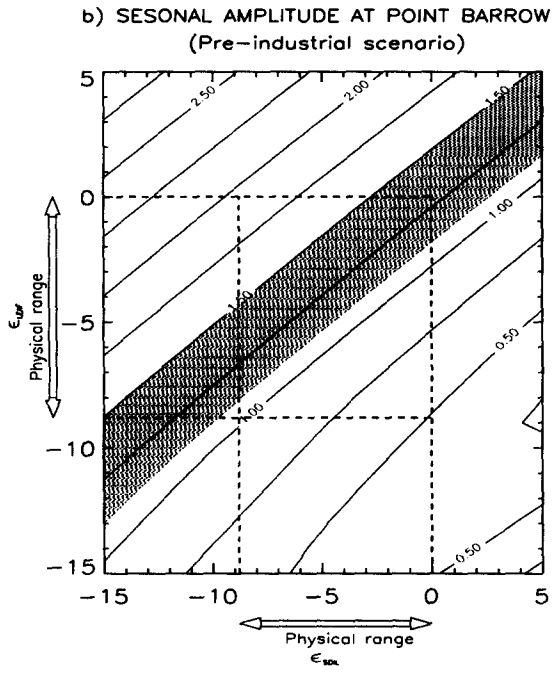

Concerning the inter-hemispheric difference (Fig. 5c) the contribution of the burning of fossil fuel is to increase by 0.3 ‰ this difference (e.g., Ciais et al. (1996b)). In this case we thus added this component to the "pre-industrial" budget in order to compare simulated differences in a realistic way to values given by the actual observations. We can also notice that fossil fuel should have induced a negative trend in the atmosphere of -0.14‰ per year. As this decrease is not observed in the measurements, other mechanisms must compensate for this effect in today's $\delta^{18}O$ budget as opposed to the "pre-industrial" simulation.

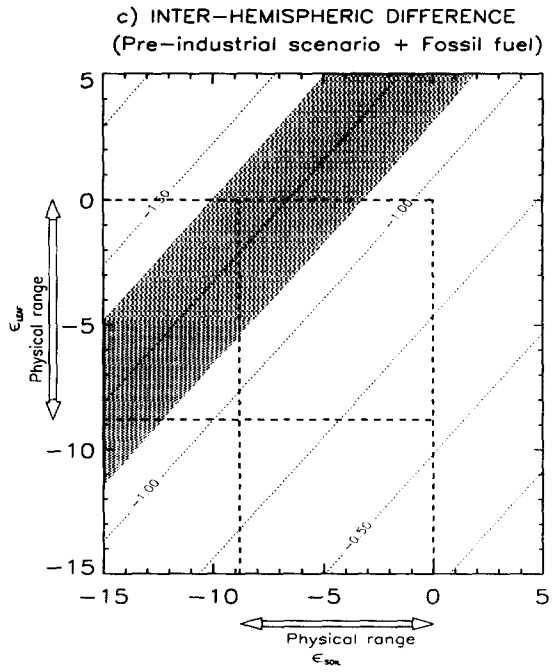

Fig. 5. Sensitivity test of $\delta^{18}O$ in atmospheric CO_2 simulated by TM2, to the fractionation factor involved during CO_2 diffusion out of soils (ϵ_{soil}) and CO_2 diffusion into/out of the leaves (ϵ_{leaf}). (a) correspond to the long term trend, (b) to the seasonal amplitude a Point Barrow (71°N, 156°W), and (c) to the inter-hemispheric difference (we took grid points between 20° and 60° for the northern hemisphere and between 20° and 60° for the southern one). (a) and (b) result only from the biospheric fluxes ("pre-industrial" scenario) while (c) includes also fossil fuel burning. The grey regions correspond to the observed range of values for each case.

In each of these plots, we defined a physical range for the fractionation factors. The lower limit (-8.8‰) corresponds to molecular diffusion with slower diffusion of $C^{18}O^{16}O$ compared to $C^{16}O_2$. On the other hand a value of zero would reflect no diffusive discrimination against ^{18}O. For soils this extreme value seems unrealistic but the closer the CO_2 production to the soil surface is, the weaker the influence of the diffusive fractionation would be because of competition between the isotopic exchange of CO_2 with water and the diffusion of CO_2 out of the soil (Hesterberg and Siegenthaler, 1991).

The main feature that comes out of these graphs is a large sensitivity of the three quantities to the fractionation factors. Nevertheless the long term trend presents

the largest sensitivity within the physical range defined for ϵ_s and ϵ_l, compared to the seasonal amplitude and the north minus south difference. We also notice that for the trend and the north minus south difference, the iso-lines follow the diagonal which indicates a linear response to both fractionation factors. On the other hand, the seasonal amplitude is more sensitive to ϵ_l than to ϵ_s (the slope of the iso-lines is smaller).

4.3 Discussion

By changing the two fractionation factors we can find a set of values that would give a reasonable agreement with the observations for both the amplitude and the inter-hemispheric difference. Concerning the long term trend, a different set of values would be required. Nevertheless this latter constraint also highly depends on other parameters. It is first sensitive to the mean $\delta^{18}O$ value of atmospheric CO_2 (δ_a in equations in Table 1). A change of $+1‰$ in δ_a for the calculation of the $C^{18}O^{16}O$ flux associated with the photosynthesis ($^{18}F_{leaves}$ in Eq. 3, Table 1) would induce a change of $+0.4‰$ per year in the mean long term trend. Globally the measurements of δ_a remain relatively sparse in term of spatial coverage and associated uncertainties are large, particularly over the tropics due to possible reaction between CO_2 and water in the flask samples. The trend also depends on the "stratospheric enrichment" of ^{18}O in CO_2 through isotopic exchange between CO_2 and O_3 (e.g., Yung et al. (1991)). Figure 4 plots the simulated vertical profile for the control run defined with a given "stratospheric enrichment" (solid line). In this case the isotopic exchange between CO_2 and O_3 induces a mean long term trend for $\delta^{18}O$ in atmospheric CO_2 of $+0.36‰$ yr^{-1} (see Fig. 3). The dot curve in figure 4 shows the same vertical profile for a simulation where we double the "stratospheric enrichment". The resulting profile is still in agreement with the observations of Gamo et al. (1989) and Thiemens and Jackson (1991), and in this case the contribution of the "stratospheric enrichment" to the mean long term trend is twice that in the control run: $+0.72‰$ yr^{-1}. It is still difficult to select one profile from the other because (i) the measurements of $\delta^{18}O$ in stratospheric CO_2 are lacking, (ii) the isotopic exchange between CO_2 and O_3 is still poorly understood and (iii) we know that the transport model TM2 overestimates vertical mixing between the troposphere and the stratosphere (the tropopause is located at too high altitudes). The range of uncertainty for δ_a and for the "stratospheric enrichment" are thus large enough to fulfill the trend constraint with different sets of values within the physical range for the fractionation factors ϵ_s and ϵ_l. The two other constraints (amplitude and inter-hemispheric difference) could be fulfilled with only one set of values for ϵ_s and ϵ_l, but this would lead to a fairly low discrimination of ^{18}O during CO_2 diffusion through leaves.

Table 1. Equations for exchanges of oxygen isotope of CO_2 with terrestrial ecosystems.

EQUATIONS

Notation : δ and δ-anomalies (δ^*)

$$\delta_i = \left(\frac{(^{18}O/^{16}O)_i}{(^{18}O/^{16}O)_{PDB-CO_2}} - 1\right) 10^3 \;;\; \delta_i^* = \frac{C_i(\delta_i - \delta_{bg})}{\sum_i C_i} \quad (1)$$

Isotopic equilibrium with water :

$$COO + H_2{}^{18}O \longleftrightarrow CO^{18}O + H_2O$$

$$with\ \alpha_{equ} = \frac{(^{18}O/^{16}O)_{eq2}}{(^{18}O/^{16}O)_{H_2O}} = f(T) \quad (2)$$

LEAF exchange of ^{18}O :

$$^{18}F_{leaves} = -\alpha_l R_a F_{al} + \alpha_l R_l F_{la}$$

$$with\ A = -F_{al} + F_{la} \quad (3)$$

SOIL exchange of ^{18}O :

$$^{18}F_{soils} = -\alpha_s R_s F_{resp} \quad (4)$$

OCEAN exchange of ^{18}O :

$$^{18}F_{ocean} = -\alpha_w R_a F_{ao} + \alpha_w R_o F_{oa}$$

$$with\ F_{oa} - F_{ao} = Kex\ \Delta pCO_2 \quad (5)$$

Global mass balance (with the δ-notation) :

$$C_a\, d\delta_a/dt = A\,\Delta_A + R_{soils}(\delta_s - \delta_a + \epsilon_s) + \epsilon_w(F_{ao} - F_{oa}) + F_{oa}(\delta_o - \delta_a) \quad (6)$$

SYMBOLS

A	Net rate of CO_2 assimilation
F_{resp}	CO_2 released by soil and plant respiration
$^{18}F_{soils}$	Flux of $C^{18}O^{16}O$ from soils
$^{18}F_{leaves}$	Flux of $C^{18}O^{16}O$ from leaves
$^{18}F_{ocean}$	Flux of $C^{18}O^{16}O$ from ocean
F_{al}	Gross flux of CO_2 into the leaves
F_{la}	Gross flux of CO_2 out of the leaves
F_{ao}	Gross flux of CO_2 into the ocean
F_{oa}	Gross flux of CO_2 out of the ocean
Kex	exchange coefficient for CO_2 between the atmosphere and sea-surface water
ΔpCO_2	Difference in partial pressure of CO_2 between the air and sea water
α_{equ}	Isotopic equilibration factor between CO_2 and H_2O
α_s	CO_2 fractionation factor for diffusion out of soil
α_l	CO_2 fractionation factor for diffusion into/out of the leaves
α_w	Fractionation factor for CO_2 during dissolution and diffusion in water
ϵ_s, ϵ_l, ϵ_w	$(\alpha_i - 1) \cdot 10^3$ (for i = s,l,w)
R_s	$^{18}O/^{16}O$ ratio of CO_2 in isotopic equilibrium with soil moisture
R_l	$^{18}O/^{16}O$ ratio of CO_2 in isotopic equilibrium with chloroplast water
R_o	$^{18}O/^{16}O$ ratio of CO_2 in isotopic equilibrium with sea-water
R_a	$^{18}O/^{16}O$ ratio of atmospheric CO_2: zonal fit (Loess curve) to the monthly mean $\delta^{18}O$ values derived from the NOAA-CU observations
δ_a, δ_s, δ_o	isotopic ratio in δ units for atmosphere, soil, ocean
δ_{bg}	"background" atmospheric δ (set up to $0.0‰$)
δ_i	simulated δ field corresponding to process i
Δ_A	Discrimination against ^{18}O (compared to ^{16}O) during net CO_2 assimilation by photosynthesis (Farquhar et al., 1993)
Ca	Number of moles of CO_2 in the atmosphere
C_i	Concentration field corresponding to process i
PDB-CO_2	CO_2 derived from Pee Dee Belemnite calcite

5 Conclusion

This short study discusses the sensitivity of the seasonal amplitude, the north minus south difference and the long term trend of $\delta^{18}O$ in atmospheric CO_2 to the fractionation factors for diffusion of CO_2 out of the soil and into/out of the leaves. Variation of these factors within the physical range induce large variations of the atmospheric $\delta^{18}O$ signal. The long term trend is nevertheless the most sensitive. But the simulation of this quantity highly depends on others processes such as the "stratospheric enrichment" of ^{18}O in CO_2 (discussed above) and on the isotopic composition of the water in the leaves. The $\delta^{18}O$ of the water inside the chloroplast is fairly sensitive to the $\delta^{18}O$ of the water vapor inside the canopy. As a first test we changed the $\delta^{18}O$ of water vapor to the extreme case where it is set to the $^{18}O/^{16}O$ ratio of precipitation (i.e., assuming that vapor in the canopy is constituted by $100^o/_o$ of plant transpiration). In this case we obtain a positive long term trend with only little changes of the seasonal amplitude and the latitudinal gradient.

Acknowledgements. We would like to thanks the ESCOBA project, PNEDC-France for the financial support of this research.

References

Ciais, P., Denning, A. S., Tans, P. P., Berry, J. A., Randall, D. A., Collatz, G. J., Sellers, P. J., White, J. W., Trollier, M., Meijer, H. A. J., Francey, R. J., Monfray, P., and Heimann, M., A three dimensional synthesis study of $\delta^{18}O$ in atmospheric CO_2, Part I : Surface fluxes, *J. Geophys. Res., in press*, 1996a.

Ciais, P., Tans, P. P., Denning, A. S., Francey, R. J., Trollier, M., Meijer, H. J., White, J. W., Berry, J. A., Randall, D. A., Collatz, J. J. G., Sellers, P. J., Monfray, P., and Heimann, M., A three dimensional synthesis study of $\delta^{18}O$ in atmospheric CO_2, Part II : Simulations with the TM2 transport model, *J. Geophys. Res., in press*, 1996b.

Craig, H. and Gordon, A., Deuterium and Oxygen-18 variations in the ocean and the marine atmosphere, in *Stable isotopes in Oceanic Studies and Paleotemperatures*, edited by Laboratory of geology and Nuclear Science, Pisa, 1965.

Erickson, D. J., A stability dependent theory for air-sea exchange, *J. Geophys. Res., 98*, 8471–8488, 1993.

Farquhar, G. D., Lloyd, J., Taylor, J. A., Flanagan, L. B., Syvertsen, J. P., Hubick, K. T., Wong, S., and Ehleringer, J. R., Vegetation effects on the isotope composition of oxygen in atmospheric CO_2, *Nature, 363*, 439–443, 1993.

Fowler, L. A., Randall, D. A., and Rutledge, S. A., Liquid and ice cloud microphysics in the CSU General Circulation Model. Part I : Model description and simulated microphysical processes, *J. Climate, 9*, 489–529, 1996.

Francey, R. J. and Tans, P., Latitudinal variation in oxygen-18 of atmospheric CO_2, *Nature, 327*, 495–497, 1987.

Francey, R. J., Robbins, F. J., Allison, C. E., and Richards, N. G., The CSIRO global survey of CO_2 stable isotopes, in *Baseline Atmospheric Research Program (Australia) 1988*, edited by S. R. Wilson and G. P. Ayers, Department of Administrative Services/Bureau of Meteorology and CSIRO Division of Atmospheric Research, 1990.

Gamo, T., Tsutsumi, M., Sakai, H., Nakazawa, T., Tanaka, M., Honda, H., and Kubo, H., Carbon and oxygen isotopic ratios of carbon dioxide of a stratospheric profile over Japan, *Tellus, 41B*, 127–133, 1989.

Heimann, M., The global atmospheric tracer model TM2 : Model description and user manual, Tech. Rep. 10, Max Planck Institut fur Meteorologie, Hamburg, 1995.

Hesterberg, R. and Siegenthaler, U., Production and stable isotopic composition of CO_2 in a soil near Bern, Switzerland, *Tellus, 43B*, 197–205, 1991.

Jouzel, J., Russell, G. L., Suozzo, R. J., Koster, R. D., White, J. W. C., and Broecker, W. S., Simulations of the HDO and $H_2{}^{18}O$ atmospheric cycles using the NASA/GISS general circulation model : The seasonal cycle for present-day conditions, *J. Geophys. Res., 92*, 14739–14760, 1987.

Keeling, C. D., The concentration and isotopic abundance of carbon dioxide in rural and marine air, *Geochimica et Cosmochimica Acta, 24*, 277–298, 1961.

Liss, P. S. and Merlivat, L., Air-sea gas exchange rates: Introduction and synthesis, in *The Role of Air-Sea Exchange in Geochemical Cycling*, edited by P. Buat-Ménard, pp. 113–127, D. Reidel, 1986.

Maier-Reimer, E., Geochemical cycles in an ocean general circulation model. preindustrial tracer distributions, *Global Biogeoch. Cycl., 7*, 645–677, 1993.

Randall, D. A. and Pan, D. M., Implementation of the Arakawa-Schubert parameterization with a prognostic closure, in *The Representation of Cumulus Convection in Numerical Models*, edited by K. Emanuel and D. Raymond, pp. 137–144, American Meteorological Society, 1993.

Randall, D. A., Shao, Q., and Moeng, C.-H., A second-order bulk boundary-layer model, *J. Atmos. Sci., 49*, 1903–1923, 1992.

Randall, D. A., Dazlich, D. A., Zhang, C., Denning, A. S., Sellers, P. J., Tucker, C. J., Bounoua, L., Berry, J. A., Collatz, G. J., Field, C. B., Los, S. O., Justice, C. O., and Fung, I., A revised land surface parameterization (SiB2) for atmospheric GCMs. Part III : The greening of the Colorado State University General Circulation Model, *J. Climate, 9*, 738–763, 1996.

Sellers, P. J., Mintz, Y., Sud, Y. C., and Dalcher, A., A simple biosphere model (SiB) for use within general circulation models, *J. Atmos. Sci., 43*, 505–531, 1986.

Sellers, P. J., Randall, D. R., Collatz, G. J., Berry, J. A., Field, C. B., Dazlich, D. A., Zhang, C., Collelo, G. D., and Bounoua, L., A revised land surface parameterization (SiB2) for atmospheric GCMs. Part I : Model formulation, *J. Climate, 9*, 676–705, 1996.

Six, K. D. and Maier-Reimer, E., Effect of plankton dynamics on seasonal carbon fluxes in an ocean general circulation model., *Global Biogeoch. Cycl., in press*, 1996.

Thiemens, M. H. and Jackson, T., Oxygen isotope fractionation in stratospheric CO_2, *Geophys. Res. Letters, 18*(4), 669–672, 1991.

Trolier, M., White, J., Tans, P., Masarie, K., and Gemery, P., Monitoring the isotopic composition of atmospheric CO_2 : measurements from the NOAA global air sampling network, *Global Biogeoch. Cycl., accepted*, 1996.

Yung, Y. L., DeMore, W. B., and Pinto, J. P., Isotopic exchange between carbon dioxide and ozone via $o(^1d)$ in the stratosphere, *Geophys. Res. Letters, 18*(1), 13–16, 1991.